

Structural analysis of dapped-end beams through machine learning techniques

V. Picciano, G. Santarsiero, A. Masi & A. Digrisolo
School of Engineering, University of Basilicata, Potenza, Italy

ABSTRACT: Dapped-end beams (or half-joints) are extensively used in both reinforced concrete bridge structures and roofs and flooring for prefabricated buildings. Due to their geometric configuration, they represent discontinuity regions where high stresses concentrate. Therefore, it is crucial to evaluate the load-bearing capacity of these elements which may depend on various parameters, such as the strength of materials, the quantity and the different layouts of the used reinforcements which also significantly influence their failure mode. For this purpose, a literature review led to the creation of an experimental tests database used to conduct an in-depth statistical analysis, considering the influence of various parameters on the ultimate load capacity and failure mode of dapped-end beams. The collected database has been also used to train a regression model with supervised machine learning techniques in order to predict the ultimate capacity of dapped-end beams.

1 INTRODUCTION

Dapped-end beams have some advantages related to construction speed as connections are represented by half-joints (Figure 1) which facilitate the installation operations. In bridge structures, dapped-end beams are used as part of the cantilever bridges (also called Gerber bridges) for their capability of absorbing small settlements along with a convenient stress distribution. Geometrical details of dapped-end regions make them disturbed regions in which the Bernoulli theory cannot be applied to evaluate stresses and carry out the due safety checks, requiring purposely set-up assessment methods.

In fact, the load-bearing capacity of dapped-end beams can be assessed through different analytical and numerical methods. For example, strut-and-tie models (Mattock 2012, EN 1992-2 2005), eventually accounting for deterioration (Desnerck et al. 2018), are among the lower-bound methods, capable of providing conservative assessments.

The strut-and-tie method (STM) is based on the definition of a truss model that must be consistent with the behavior of dapped-ends observed during experiments in order to idealize the force flow in the recessed part of the beam end. STM trusses that better approximate the force flow in a structural component allow the design of an efficient reinforcement layout increasing the specific failure load and minimizing the occurrence of cracks under the service loads (Mattock 2012). Eurocode 2 (EN 1992-2 2005) provides two alternative models and related reinforcement layouts (one considering only horizontal and vertical bars while the other accounts for the inclined reinforcement also) which can be combined to evaluate to overall strength of a half-joint.

A design method is also reported in the PCI Design Handbook (2010) mainly devoted to precast elements belonging to buildings. This method is based on an experimental investigation in which several potential failure modes were highlighted. In particular, the safety checks of different reinforcement devices are made concerning five specific possible failure modes which can affect both the undapped and the dapped regions of the half-joint. The PCI method has some limitations compared to STM since does not consider inclined rebars and is valid for cases where the shear

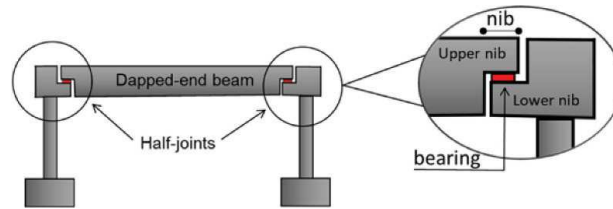


Figure 1. Typical dapped-end beam and half-joint detail.

span-to-depth ratio does not exceed 1.0. For these reasons, it is hardly helpful in the assessment of existing dapped-end elements.

Besides STM and PCI methods, kinematic methods can be used to predict the peak strength of half-joints. These methods assume that the failure mode is governed by the opening of a crack according to a selected pattern (e.g. diagonal cracking starting from the re-entrant corner) and impose that the static equilibrium is guaranteed by the steel crossing it. For example, the model proposed by Rajapakse et al. (2021) is based on the knowledge of the crack angle developing from the re-entrant corner assuming that the failure is governed by flexure stress. Moreover, the model considers the crack width as well as the amount of dapped-end reinforcement, along with the crack length and the rotation about the crack tip. This model was applied to a database of 47 experimental tests providing good prediction results compared to actual values.

A further option to assess the capacity of half-joints is represented by numerical methods consisting of refined finite element models based on nonlinear fracture mechanics (Bazant & Oh 1983). Moreover, there are modelling procedures which can explicitly account for corrosion propagation inside the member during a given period, allowing to perform durability analyses (Santarsiero et al. 2021).

In order to deepen the structural behaviour of dapped-end beams, this study describes a literature review on experimental tests of such elements, leading to the construction of a database of 210 specimens. Following a brief description of the half-joints' typical details and failure modes, a statistical analysis of the main collected parameters was conducted to observe their variability and highlight correlations, such as those between specific failure modes and certain reinforcement layouts. Finally, the database was used to train different regression models using supervised machine learning techniques to predict the ultimate strength of the specimens. These techniques helped identify the best-performing regression model that can be employed to quickly assess dapped-end beams.

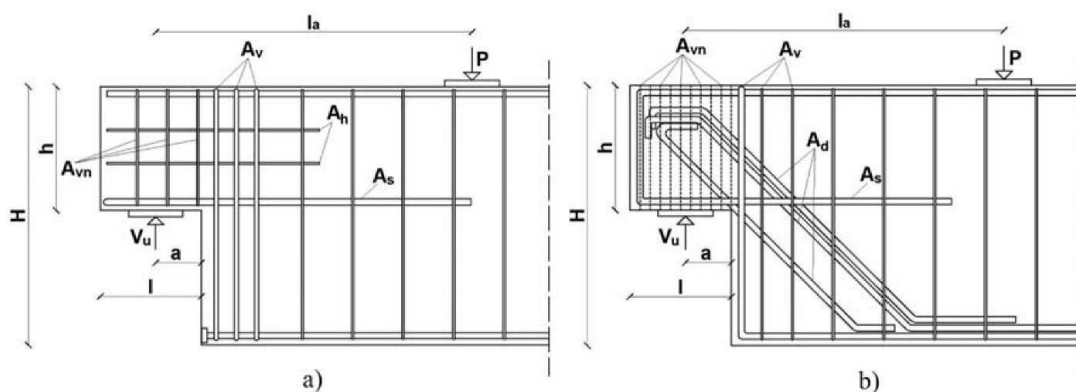


Figure 2. Different half-joint reinforcement layouts a) involving only vertical and horizontal reinforcement and b) also with inclined ones.

2 TYPICAL DETAILS AND FAILURE MODES

Due to their geometry, half-joints represent a discontinuity zone from the perspective of stress distribution, and, as previously illustrated, they require specific design and assessment methods. From a construction detailing point of view also, they represent singular elements

since the arrangement of reinforcements necessary for external load absorption can vary. In particular, considering both the upper and lower nib (Figure 1) as statically equivalent, the two most commonly used reinforcement layouts are illustrated in Figure 2.

Figure 2a illustrates a reinforcement layout mainly related to building structures, where only vertical and horizontal rebars are used. In this case, the absorption of external vertical forces occurs through the formation of an inclined concrete strut in the nib, which, for equilibrium purposes, requires the presence of a vertical tie, represented by the vertical stirrups A_v , and a horizontal tie through the presence of the A_s reinforcements, to which the contribution of horizontal secondary reinforcements A_h can be added, arranged within the nib as illustrated. The nib vertical stirrups A_{vn} have the purpose of confining the inclined concrete strut, thereby increasing its resistance and ductility. Therefore, the reinforcements form a truss mechanism, allowing for the absorption of external loads.

The alternative layout depicted in Figure 2b also involves the presence of inclined reinforcements A_d , providing an additional contribution to the truss mechanism. In particular, this second type of reinforcement layout is widely used within the Gerber saddles of existing bridges, especially in Europe. Inclined reinforcements, besides enhancing the overall half-joint's strength (Desnerck et al. 2016), also limit re-entrant corner cracking under service loads thus limiting the ingress of polluting agents such as chlorides, which can cause reinforcement corrosion (Santarsiero & Picciano 2023).

As for the dapped-end's ultimate behaviour, it is worth emphasizing that there can be different collapse modes depending on the adopted reinforcement layout. In particular, according to the PCI Design Handbook (2010), five potential failure modes are observed in half-joints under vertical loads (Figure 3). Mode 1 involves nib vertical cracking due to flexure and axial tension; mode 2 results from direct shear at the junction of the nib and the undapped region; mode 3 is caused by re-entrant corner diagonal tension; mode 4 represents nib shear failure, and mode 5 is due to diagonal tension in the undapped portion.

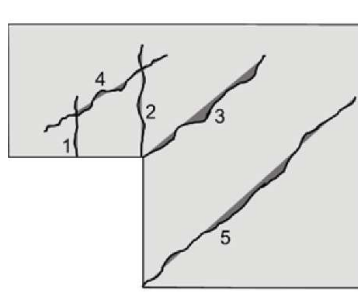


Figure 3. Possible half-joint failure modes according to the PCI Design Handbook (2010).

3 EXPERIMENTAL CAMPAIGNS AND DATABASE COLLECTION

In order to characterize the typical detailing, the failure modes and structural performances, a review of experimental research on half-joints has been conducted and partially illustrated in Santarsiero et al. (2023). This review activity allowed the collection of 147 experimental tests on dapped-end beams which have been recently updated to a total of 210, gathering information from 22 different research projects in the literature, briefly described in the following, for which several parameters were recorded. In particular, the amount and yielding stress of steel reinforcement at any position (stirrups, main vertical and horizontal, inclined) was annotated as well as the detailed geometry, concrete grade and, finally, the load test scheme along with the experimental peak load and failure type obtained during the test.

Mattock & Chan (1979) tested 8 dapped-end beam specimens all provided with the same geometry and different amounts of reinforcement in the vertical and horizontal direction along the re-entrant corner. In Kumaraguru (1992), 12 dapped-end beams were tested to find the capacity of the nibs for different locations of the support reaction and therefore with

different values of the shear span-to-depth ratio. Lu et al. (2003) conducted an experimental program to study the behaviour of high-strength concrete dapped-end beams testing 12 specimens with the same geometry and different detailing and concrete strength. The effect of different amounts of principal horizontal and vertical reinforcement, the shear span-to-depth ratio and the concrete strength on the specimens' shear capacity was analysed by Lin et al. (2003) testing 24 high-strength concrete dapped-end beams. Tests on 18 dapped-end specimens were selected from Wang et al. (2005). In this paper, the specimens' resistance was investigated as a function of dapped-end height, the reinforcement layout, in particular related to the presence of inclined rebars which is found to influence the load-bearing capacity. Taher (2005) experimentally tested 3 specimens having identical geometry but different detailing. They were used as control specimens in an experimental campaign devoted to testing various strengthening techniques. 7 specimens were selected from Herzinger (2008) that investigated the efficiency of studs with single or double heads for reinforcing the dapped-ends. This latter prevents premature failure caused by inadequate anchorage of conventional reinforcement and an experimental campaign was set up in order to make a comparison with the behaviour of conventionally reinforced dapped-end beams. Lu et al. (2012) tested 24 specimens having different geometry, concrete grades and amount of reinforcement in order to find the influence of these parameters on the load capacity and failure mode. Ahmad et al. (2013) tested 4 reinforced concrete dapped-end beams divided into two groups with different depth values. The research aimed to investigate the effectiveness of STM in predicting the failure load finding that, in the case of lower depth dapped-end beams, unconservative solutions were obtained. Moreno-Martínez & Meli (2014) conducted a research program to evaluate the performance of a dapped-end solution for a railway bridge with respect to both service and ultimate loads, to explore solutions that can enhance the component's performance. The study conducted by Mata-Falcón (2015) provides a set of 60 tests on dapped-ends (among which 8 have been selected for the database), corresponding to 30 different configurations in which parameters such as the amount and layout of reinforcement were studied. Lu et al. (2015) investigated the shear strength of 24 reinforced concrete dapped-end beams with shear span-to-depth ratios larger than unity. Aswin et al. (2015) experimentally investigated the shear response of 4 large-scale RC dapped-end specimens to find out the influence of the amount of nib reinforcements, the main flexural reinforcements, and concrete type at the dapped-end area. Atta & Taman (2016) studied the effectiveness of strengthening systems applied to dapped-end beams. Therefore, they also tested a control specimen. Desnerck et al. (2016) studied the behaviour of 4 half-joint specimens to find out the effect of local reductions in reinforcing bars and cracking in the anchorage zone on the load-bearing capacity. Desnerck et al. (2018) studied the tuning of STMs for deteriorated RC half-joints through an experimental campaign. 2 specimens out of 12 were used as control specimens and were included in this database. Hussain & Shakir (2019) tested several dapped-end specimens two of which are collected in the database. The study aimed to find the effect of repeated loads and the influence of increased shear span-to-depth ratio. Mata-Falcón et al. (2019) proposed simplified strut-and-tie models which were experimentally validated through static tests on 15 dapped-end beam specimens. The database also considered 24 dapped-end beams among the 27 specimens experimentally tested by Mohamed et al. (2020). They investigated the effect of a shear span-to-depth ratio larger than 1.0 finding that the PCI approach for the evaluation gave an underestimation with respect to experimental capacity values. The study conducted by Rajapakse et al. (2022) involved the execution of 8 large-scale dapped-end tests to investigate the influence of the amount of reinforcement in terms of the ratio of dapped-end horizontal to vertical reinforcement area. This variable was correlated with the dapped-end's resistance, crack control, and rotation capacity. Di Carlo et al. (2023a,b) investigated the impact of reinforcement corrosion on the strength and failure mode through the implementation of an experimental campaign on dapped-end beams, of which 4 control specimens have been selected for this database.

In summary, most of the experimental research programs here investigated are devoted to analysing the effect of different shear span-to-depth ratios, alternative reinforcement layouts and amounts as well as the influence of concrete grades adopted. Therefore, the database has a wide variability of governing parameters to allow an in-depth statistical analysis.

First of all, a brief overview of the collected parameters' variability is illustrated. In particular, referring to the geometric scheme depicted in Figure 2, Table 1 reports the minimum, maximum and mean values also with the standard deviation of the main specimens' geometric features, namely the dapped-end's width b , the ratio between the nib depth and the full beam depth h/H , the nib length-to-nib depth ratio llh , the shear span-to-depth ratio alh and the lever arm adopted during the experimental test in terms of l_a/H ratio.

Furthermore, over 60% of the specimens exhibit a full depth exceeding 500 mm, a share of 25% less than 500 mm and upper than 250 mm, and only 13% have a lower depth. As indicated by the mean value in Table 1, the majority of specimens have an alh ratio below 1, while only 9% fall into the category where it exceeds unity. Turning to the strength characteristics of the specimens, the variability in both concrete and steel strength was analysed. Specifically, most of the specimens exhibit a mean value of cylindrical concrete compressive strength exceeding 20 MPa, and a share of 45% is classified as high-strength concrete specimens with $f_c > 40$ MPa. The steel used for tested dapped-ends has different grades for horizontal, vertical and stirrup rebars. Considering the average strength value among the different grades used for each specimen, more than 50% of them have a rather low yielding strength ($f_{ym} < 320$ MPa), 40% have $320 < f_{ym} \leq 450$ MPa and only 8% have a yielding strength upper than 450 MPa.

Regarding the failure mode, in 204 out of 210 tests included in the database, it was possible to attribute the collapse mode to one of the 5 types indicated in the PCI Design Handbook (2010) or a combination of them. Considering that only 36 tests are provided with inclined reinforcements, while 168 present only vertical and horizontal rebars, it has been observed that in the former case, the most frequent failure mode (30%) is associated with a combination of modes 3 and 4 (Figure 3), followed by mode 5 (22%) and mode 3 (13.9%), while pure mode 4 is almost absent. In the absence of inclined reinforcements, the tested dapped-ends mostly failed through modes 3 and 4 or a combination of them. Therefore, the presence of inclined reinforcements seems to prevent failure mode 4 related to shear stresses in the nib.

Table 1. Boundary range of the specimens' geometric features.

Parameter	Min	Max	Mean	St.dev
b (mm)	120	1000	208.9	99.2
h/H (-)	0.43	0.77	0.53	0.07
llh (-)	0.46	2.50	1.20	0.47
alh (-)	0.13	1.33	0.59	0.27
l_a/H (-)	0.64	3.79	1.32	0.64

4 DATABASE ANALYSIS AND DISCUSSION

Data from individual experimental tests were employed to train a Machine Learning algorithm aimed at predicting the load-bearing capacity of any half-joint. In fact, supervised learning techniques take a known set of input data (the training set) and known responses to the data (output), and train a model to generate reasonable predictions employing new input data. These techniques are widely used in the field of civil engineering, particularly to predict specific responses, representing a reliable alternative to analytical models based on the use of a few control parameters that may not be representative of the whole studied phenomenon (Koya et al. 2022).

In this case, supervised learning techniques were employed to train a regression algorithm based on information from 210 literature experimental tests on dapped-ends. The input data are geometric and mechanical parameters, as well as construction details in terms of reinforcement layouts and amount. The output data consisted of the ultimate strength of each test.

Figure 4 provides a detailed illustration of the input and output parameters used for model training. Specifically, 10 input parameters were considered, involving geometric parameters

such as dapped-end width b , nib depth h , full beam depth H and shear span a . Regarding mechanical parameters and construction details, concrete strength f_c was taken into account, along with the strength's contributions of each reinforcement layout. This involved the product of the reinforcement area and the average yielding strength of the corresponding steel rebars. Therefore, referring to the scheme in Figure 2, the strength associated with the main horizontal bars is calculated as $R_s = A_s \cdot f_{ym,s}$, the contribution of the main vertical stirrups is $R_v = A_v \cdot f_{ym,v}$, the inclined reinforcements contribute $R_d = A_d \cdot f_{ym,d}$, and finally, the contribution of secondary horizontal and vertical stirrups in the nib are determined as $R_h = A_h \cdot f_{ym,h}$ and $R_{vn} = A_{vn} \cdot f_{ym,vn}$, respectively.

The training of the predictive algorithm was carried out using the MATLAB software (The MathWorks Inc. 2023a), specifically through the Statistics and Machine Learning Toolbox (The MathWorks Inc. 2023b). This toolbox allows for the utilization of the Regression Learner App, which interactively trains, validates, and tunes regression models.

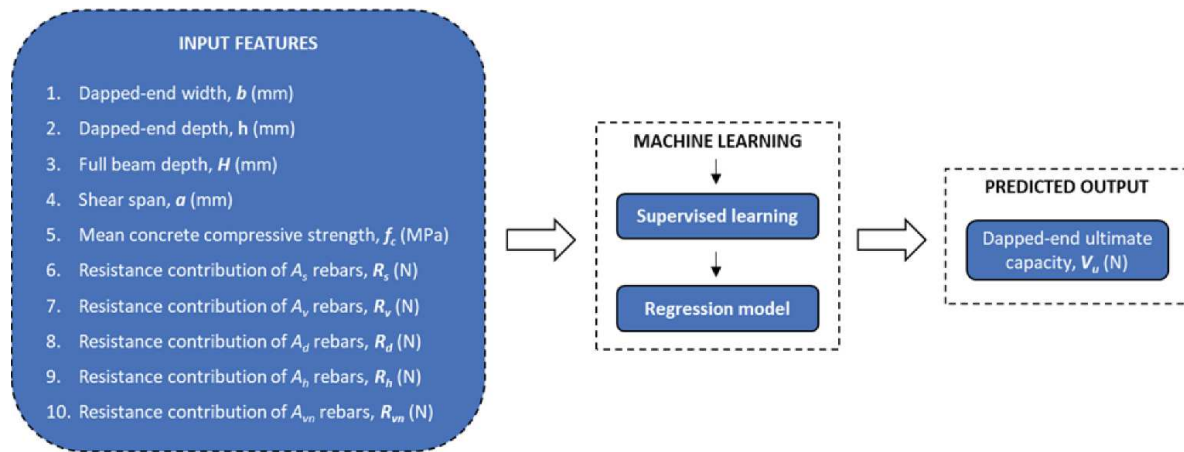


Figure 4. Adopted input and output variables for predicting the dapped-end ultimate capacity with machine learning algorithms.

The entire database of 210 observations was divided into a training set containing 80% of the samples (168 samples) and a test set comprising the remaining 20% (42 samples). This operation was performed automatically within the application to randomly partition the database based on the provided size. This latter ensures the random selection of observations used for the test dataset and avoids any bias introduced by manual selection.

The training set represents the data on which the regression model is trained, while the test set is used to check the accuracy of predictions and other statistical measures, aiming to prevent inaccurate results due to overfitting of data.

The Regression Learner App allowed for training and evaluating the predictive capability of different regression models, including Linear Regression, Nonlinear Regression, Gaussian Process Regression Model, SVM Regression, Generalized Linear Model, and Regression Tree. In order to identify the model with the best predictive capacity, the coefficient of determination R^2 was employed as a performance indicator. It can be calculated as follows:

$$R^2 = 1 - \frac{\sum_{i=1}^N [V_{upredicted} - V_{uexperimental}]^2}{\sum_{i=1}^N [V_{upredicted} - \bar{V}_{uexperimental}]^2} \quad (1)$$

Based on this performance indicator, the regression model with the best predictive capability is the Rational Quadratic Gaussian Process Regression (GPR), which exhibited an R^2 value of 0.984 for the test dataset and a value of 0.958 for the training set.

In particular, the GPR model represents a nonparametric regression method designed to accommodate more complex regression curves without specifying the relationship between the response and the predictors through a predetermined regression function (Rasmussen & Williams 2006). Figure 5 shows the results of the trained model in terms of comparison between

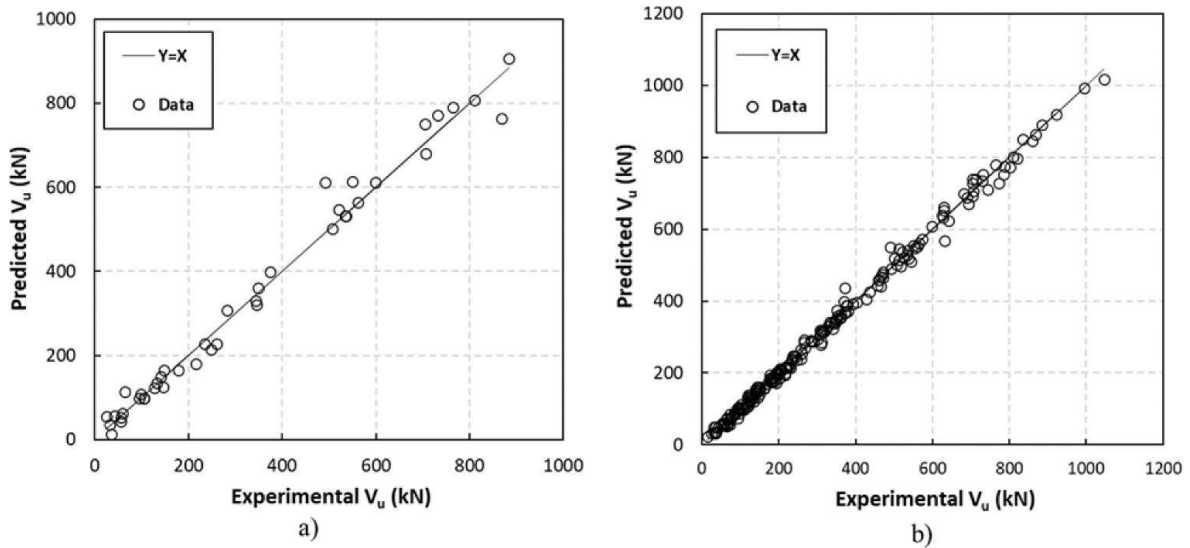


Figure 5. Comparison of the experimental and predicted dapped-end ultimate capacity a) for the test dataset only and b) considering all data.

the experimental values of dapped-end ultimate capacity and the predicted ones, considering only the test dataset (Figure 5a) as well as the prediction obtained based on the entire dataset of 210 specimens (Figure 5b). Although the trained model has shown a rather high value of the performance indicator R^2 , it is worth highlighting that the accuracy of the model depends on the size of the dataset. On the other hand, this study has shown a rapid method which can be useful to obtain an accurate response for purposes such as condition assessment and preventive retrofitting measures for existing half-joints.

To make the predictive model available, a repository (https://github.com/Picciano-unibas/ML_HalfJoints) has been created, which includes the MATLAB code. This code can be used to retrain the model based on a new database, structured as illustrated in this study. Additionally, a “struct” array is included in the repository, containing the trained model, which can be employed to make predictions with new input data.

5 CONCLUSIONS

This paper is aimed at studying the half-joints’ structural behaviour through the collection of a series of experimental results by various authors, allowing to building of a database including more than 200 tests. From each test, the main specimens’ features were taken such as geometrical data, material properties related to concrete and reinforcing steel as well as regarding the amount and layout of reinforcement. These properties were represented by ten variables whose influence on the ultimate resistance of the half-joints was investigated through machine learning algorithms. These latter were aimed at predicting the load-bearing capacity of the half-joints considered in this study. The best performing algorithm was found to be the Rational Quadratic Gaussian Process Regression (GPR), which gave a high correlation between experimental and predicted strength values over both the test set and the entire dataset. The trained algorithm is freely available through a public repository and can be used for the preliminary assessment of reinforced concrete half-joints. In the future, ML classification algorithms will be used to predict the failure mode and ductility features of half-joints to provide a comprehensive analysis tool.

ACKNOWLEDGMENTS

The studies presented here were carried out as part of the activities envisaged by the Agreement between the Italian Department of Civil Protection and the ReLUIS Consortium (DPC-ReLUIS

project 2022-24, WP5-Task 5.4 “Upgrading and retrofitting interventions of existing bridges”). The contents of this paper represent the authors’ ideas and do not necessarily correspond to the official opinion and policies of DPC.

REFERENCES

- Ahmad, S., Elahi, A., Hafeez, J., Fawad, M., & Ahsan, Z. (2013). Evaluation of the shear strength of dapped ended beam. *Life Science Journal*, *10*(3), 1038–1044.
- Aswin, M., Mohammed, B. S., Liew, M. S., & Syed, Z. I. (2015). Shear failure of RC dapped-end beams. *Advances in Materials science and engineering*, 2015.
- Atta, A., & Taman, M. (2016). Innovative method for strengthening dapped-end beams using an external prestressing technique. *Materials and Structures*, *49*(8), 3005–3019.
- Bazant, Z. P., & Oh, B. H. (1983). Crack band theory for fracture of concrete. *Matériaux et construction*, *16*, 155–177.
- Desnerck, P., Lees, J. M., & Morley, C. T. (2016). Impact of the reinforcement layout on the load capacity of reinforced concrete half-joints. *Engineering Structures*, *127*, 227–239.
- Desnerck, P., Lees, J. M., & Morley, C. T. (2018). Strut-and-tie models for deteriorated reinforced concrete half-joints. *Engineering Structures*, *161*, 41–54.
- Di Carlo, F., Meda, A., Molaioni, F., & Rinaldi, Z. (2023a). Experimental evaluation of the corrosion influence on the structural response of Gerber half-joints. *Engineering Structures*, *285*, 116052.
- Di Carlo, F., Molaioni, F., Meda, A., & Rinaldi, Z. (2023b). Structural Behaviour of Gerber Half-Joints Subjected to Steel Corrosion. In *International Symposium of the International Federation for Structural Concrete* (pp. 322–331). Cham: Springer Nature Switzerland.
- EN 1992-2. (2005). Eurocode 2: *Design of concrete structures – Part 2: Concrete bridges – Design and detailing rules*. Belgium: European Committee for Standardization.
- Herzinger, R. (2008). *Stud Reinforcement in Dapped Ends of Concrete Beams*. PhD thesis, University of Calgary, Calgary, Alberta, Canada, 2008, 139–228.
- Hussain, H. N., & Shakir, Q. M. (2019). Experimental Study of the Behavior of Reinforced Concrete Beams with Composite Dapped End under Effect of Static and Repeated Loads. *International Journal of Applied Science*, *2*(1).
- Koya, B. P., Aneja, S., Gupta, R., & Valeo, C. (2022). Comparative analysis of different machine learning algorithms to predict mechanical properties of concrete. *Mechanics of Advanced Materials and Structures*, *29*(25), 4032–4043.
- Kumaraguru, P. (1992). *Strength of dapped end beams*. MSc Thesis, University of Calgary, Calgary, Alberta, Canada, 1992.
- Lin, I. J., Hwang, S. J., Lu, W. Y., & Tsai, J. T. (2003). Shear strength of reinforced concrete dapped-end beams. *Structural engineering and mechanics: An international journal*, *16*(3), 275–294.
- Lu, W. Y., Chen, T. C., & Lin, I. J. (2015). Shear strength of reinforced concrete dapped-end beams with shear span-to-depth ratios larger than unity. *Journal of Marine Science and Technology*, *23*(4), 5, 431–442.
- Lu, W. Y., Lin, I. J., & Yu, H. W. (2012). Behaviour of reinforced concrete dapped-end beams. *Magazine of concrete research*, *64*(9), 793–805.
- Lu, W. Y., Lin, I. J., Hwang, S. J., & Lin, Y. H. (2003). Shear strength of high-strength concrete dapped-end beams. *Journal of the Chinese Institute of Engineers*, *26*(5), 671–680.
- Mata-Falcón, J. (2015). *Serviceability and Ultimate Behaviour of Dapped-end Beams* (In Spanish Estudio del comportamiento en servicio y rotura de los apoyos a media madera). PhD Thesis, Universitat Politècnica de València, Valencia, 2015, 747.
- Mata-Falcón, J., Pallarés, L., & Miguel, P. F. (2019). Proposal and experimental validation of simplified strut-and-tie models on dapped-end beams. *Engineering Structures*, *183*, 594–609.
- Mattock, A. H. (2012). Strut-and-tie models for dapped-end beams. *Concrete International*, *34*(2), 35–40.
- Mattock, A. H., & Chan, T. C. (1979). Design and behavior of dapped-end beams. *PCI journal*, *24*(6), 28–45.
- Mohammed, B. S., Aswin, M., & Liew, M. S. (2020). Prediction of failure load of RC and R-ECC dapped-end beams. *Case Studies in Construction Materials*, *13*, e00433.
- Moreno-Martínez, J. Y., & Meli, R. (2014). Experimental study on the structural behavior of concrete dapped-end beams. *Engineering Structures*, *75*, 152–163.
- PCI Design Handbook. (2010). *Precast and Prestressed Concrete*. Sixth Edition.
- Rajakakse, C., Degée, H., & Mihaylov, B. (2021). Assessment of failure along re-entrant corner cracks in existing RC dapped-end connections. *Structural Engineering International*, *31*(2), 216–226.

- Rajapakse, C., Degée, H., & Mihaylov, B. (2022). Investigation of shear and flexural failures of dapped-end connections with orthogonal reinforcement. *Engineering Structures*, 260, 114233.
- Rasmussen, C. E., & Williams, C. K. (2006). *Gaussian processes for machine learning* (Vol. 1, p. 159). Cambridge, MA: MIT press.
- Santarsiero, G., & Picciano, V. (2023). Durability enhancement of half-joints in RC bridges through external prestressed tendons: The Musmeci Bridge's case study. *Case Studies in Construction Materials*, 18, e01813.
- Santarsiero, G., Masi, A., & Picciano, V. (2021). Durability of Gerber saddles in RC bridges: Analyses and applications (Musmeci Bridge, Italy). *Infrastructures*, 6(2), 25.
- Santarsiero, G., Picciano, V., & Masi, A. (2023). Structural rehabilitation of half-joints in RC bridges: a state-of-the-art review. *Structure and Infrastructure Engineering*, 1–24.
- Taher, S. D. (2005). Strengthening of critically designed girders with dapped ends. *Proceedings of the Institution of Civil Engineers-Structures and Buildings*, 158(2), 141–152.
- The MathWorks Inc. (2023a). *MATLAB version: 23.2.0 (R2023b)*, Natick, Massachusetts: The MathWorks Inc. <https://www.mathworks.com>
- The MathWorks Inc. (2023b). *Statistics and Machine Learning Toolbox: 23.2 (R2023b)*, Natick, Massachusetts: The MathWorks Inc. <https://www.mathworks.com>
- Wang, Q., Guo, Z., & Hoogenboom, P. C. (2005). Experimental investigation on the shear capacity of RC dapped end beams and design recommendations. *Structural Engineering and Mechanics*, 21(2), 221–235.